A Simple Non-Contact Optical Method to Quantify *In-Vivo* Sweat Gland Activity and Pulsation

Amy Drexelius, Daniel Fehr, Vincent Vescoli, Jason Heikenfeld, *Senior Member, IEEE*, and Mathias Bonmarin, *Senior Member, IEEE*

Abstract*—*Objective: **Most methods for monitoring sweat gland activity use simple gravimetric methods, which merely measure the average sweat rate of multiple sweat glands over a region of skin. It would be extremely useful to have a method which could quantify individual gland activity in order to improve the treatment of conditions which use sweat tests as a diagnostic tool, such as hyperhidrosis, cystic fibrosis, and peripheral nerve degeneration.** ***Methods:*** **An optical method using an infrared camera to monitor the skin surface temperature was developed. A thermodynamics computer model was then implemented to utilize these skin temperature values along with other environmental parameters, such as ambient temperature and relative humidity, to calculate the sweat rates of individual glands using chemically stimulated and unstimulated sweating. The optical method was also used to monitor sweat pulsation patterns of individual sweat glands.** ***Results:*** **In this preliminary study, the feasibility of the optical approach was demonstrated by measuring sweat rates of individual glands at various bodily locations. Calculated values from this method agree with expected sweat rates given values found in literature. In addition, a lack of pulsatile sweat expulsion was observed during chemically stimulated sweating, and a potential explanation for this phenomenon was proposed.** ***Conclusion:*** **A simple, non-contact optical method to quantify sweat gland activity *in-vivo* was presented.** ***Significance:*** **This method allows researchers and clinicians to investigate several sweat glands simultaneously, which has the potential to provide more accurate diagnoses and treatment as well as increase the potential utility for wearable sweat sensors.**

***Index Terms*—Computational model, physiological measurements, sweat sensing, thermal imaging.**

Manuscript received October 26, 2021; revised January 6, 2022; accepted February 4, 2022. Date of publication February 16, 2022; date of current version July 19, 2022. The work of authors Vincent Vescoli, Daniel Fehr, and Mathias Bonmarin was supported by ZHAW School of Enginering. This work was supported in part by the National Defense Science and Engineering Graduate Fellowship Program and in part by the Air Force Office of Scientific Research under Grant FA9550-20-1-0117. *(Corresponding authors: Jason Heikenfeld; Mathias Bonmarin.)*

Amy Drexelius is with the Novel Devices Laboratory, University of Cincinnati, USA.

Jason Heikenfeld is with the Novel Devices Laboratory, University of Cincinnati, OH 45221 USA (e-mail: heikenjc@ucmail.uc.edu).

Daniel Fehr and Vincent Vescoli are with the Sensors and Measurements Systems Lab, Zurich University of Applied Sciences, Switzerland.

Mathias Bonmarin is with the Sensors and Measurements Systems Lab, Zurich University of Applied Sciences, Winterthur, ZH 8400, Switzerland (e-mail: mathias.bonmarin@zhaw.ch).

Digital Object Identifier 10.1109/TBME.2022.3151938

I. Introduction

CURRENT methods to quantify sweat gland activity are dominated by simple gravimetric methods where a dry paper or textile disk is placed on the skin and weighed afterwards to determine the sweat absorbed over time. Gravimetric testing is non-optimal because it does not provide real time observation of the sweat response, and like other possible approaches (e.g. skin humidity [1], galvanic skin response [2], [3]) an average sweat rate is measured instead of individual gland activity. Considering that not all sweat glands are active during sweating, the ability to record sweat rate in real time and with individual gland activity is a potentially attractive approach for deeper diagnosis of diseases such as cystic fibrosis, [4] peripheral nerve degeneration [5], [6], and hyperhidrosis [7]–[9]. Furthermore, a new and improved sweat rate measurement technique would ideally be less labor intensive, would require less equipment, and would be simpler than previous approaches.

In this article, we describe a simple non-contact optical approach to sweat rate measurement which measures individual sweat gland activity in real time. This new approach utilizes infrared (IR) camera images and additional parameters, such as ambient temperature and humidity. Using the data generated, we also observe and discuss differences between natural sweating, which was observed to be pulsatile in nature, and chemically stimulated sweating, which was observed to be continuous. With these observations, we further speculate on the physiological differences between natural sweating and stimulated sweating.

II. Materials and Methods

A. Optical Device Measurement Setup

Fig. 1 schematically presents the experimental setup. A microbolometer-based infrared camera (PI 460, Optris GmbH, Berlin, Germany) equipped with a microscope objective captured the thermal radiation of the skin surface. An in-house built software (MATLAB, MathWorks, Switzerland) was used to acquire and process the IR images using the PI Imager software SDK (PI Imager, Optris GmbH, Berlin, Germany). The camera was calibrated by the supplier and provides temperature images in degrees Celsius. Emissivity of the skin was set to 0.97 [10] and the ambient temperature and humidity were entered into the software for precise temperature measurements. The images

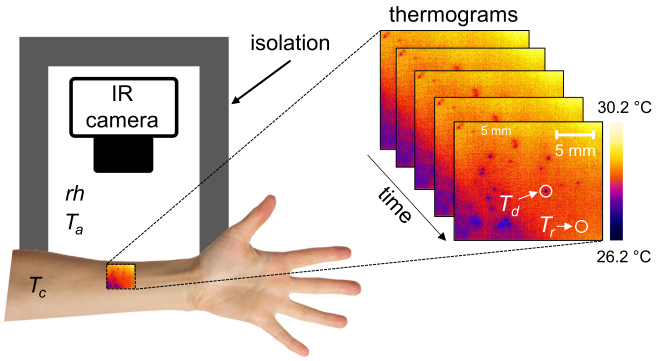

Fig. 1. Thermograms of the skin surface were recorded using an infrared camera equipped with a microscope objective (PI 460, Optris GmbH, Berlin, Germany). The camera was calibrated and gave radiometric data. Videos were acquired at a frame rate of 80 images per second to follow sweat gland dynamics over the course of several minutes. The camera and measured area were protected by isolation material to ensure constant temperature and to avoid forced convection and potential reflection into camera objective. Top right: Typical thermogram of the forearm. Individual sweat glands are clearly visible as cooler spots on the image and several sweat glands can be investigated in parallel.

were 288 × 382 pixels and the camera frame rate was 80 Hz. The noise equivalent temperature difference stated by the supplier was 40 mK. Because the frequencies of the investigated signals were low, time-dependent images were averaged and the camera framerate was decreased to 10 Hz to achieve better precision. To avoid unwanted forced convection phenomena, isolation material was used around the camera (See Fig. 1). Such material also ensured that no spurious reflections reached the camera objective. In addition, several parameters were monitored, such as the ambient temperature, T_a, and relative concentration of water vapor, rh (AQ Minion, Sensirion AG, Stäfa, Switzerland). Body core temperature, T_c (blood temperature of the subject) was also monitored (Thermoscan, Braun, Germany). To quantify the sweat rate of specific glands, a reference temperature T_r was measured away from the sweat gland in a homogeneous region as well as the minimal temperature at the location of the sweat gland (drop temperature T_d) on each thermogram (see Fig. 1). The temperatures T_r and T_d, together with the additional parameters (T_a, T_c, rh), were used to calculate the sweat rate using computational modeling. To measure potential sweat rate pulsation, the temperature at the location of the sweat gland was plotted versus time.

B. Subject Sweat Testing Protocol

Two different testing procedures were performed: i) exercise stimulated sweating (natural sweating), and ii) chemically stimulated sweating. Several healthy subjects, male and female, aged between 21 to 42, were investigated in this study. Five subjects were tested without using any chemical stimulation (on palm, forearm, and fingers), and three subjects were tested with the chemical stimulation (only on the forearm). Before any measurements were taken, all subjects were acclimatized for at least 15 minutes in the testing room.

In the case of exercise stimulated sweating, subjects were then asked to vigorously exercise (jogging, pushups, etc.) for ten minutes until sweating was induced. The optical technique was then used to record the activity of sweat glands on several locations.

In the case of chemically stimulated sweating, carbachol gels were used to iontophoretically stimulate the sweat glands. Carbachol was chosen for stimulation because it is optimal for extended periods of sweat generation. This is because it is extremely resistant to breakdown by acetylcholinesterase (about 107 times slower to metabolize than its 'natural' corresponding molecule acetylcholine), and therefore remains in the synaptic cleft and interacts with acetylcholine receptors for extended periods of time [12], [13]. The carbachol used in this study was purchased from Sigma Aldrich (part no. 1092009-200MG). The gel discs were prepared using 1% carbachol and 3% agarose, by weight, in deionized water, using the same process as in previous studies [12], [13]. The carbachol/agarose solution was heated to 150 °C and stirred for 30 minutes. The temperature was then dropped to 80 °C and the solution was reconstituted to the original volume to compensate for fluid lost to evaporation. The solution was then stirred for 30 additional minutes at this temperature to ensure that the solution was homogeneous, and then cast into disc molds (15 mm diameter × 5.8 mm height), which were made of laser cut acrylic. The filled molds were then placed into a refrigerator at approximately 4 °C for about two hours to set. The carbachol discs were then pressed out of the molds and placed into bags containing 1% carbachol in deionized water for storage. Sweat stimulation using iontophoresis was performed using a commercial unit (Wescor Nanoduct Model 1030). Before iontophoresis was performed, the stimulation site (underside of forearm) of each subject was cleaned with Isopropyl Alcohol (IPA) and deionized water to remove skin contaminants. Then, carbachol gel discs were taken out of the storage solution and placed into the electrode holders of the Nanoduct. Each of the gel electrodes (anode and cathode) was then strapped onto the arm (about 1 cm apart) using an elastic band. The full standard dosage using the Nanoduct device was delivered (42 mC · cm^{-2}) into the forearm of each subject. Before further testing was conducted, it was verified that carbachol stimulation did not cause any significant temperature changes of the skin on the testing site which may have affected sweat gland activity. No additional stimulations were performed on the same subject within 24 hours for safety purposes. It should be noted that the work done in this study was all conducted under the University of Cincinnati approved IRB protocol 2020-0604. After stimulation of the sweat glands was complete, the optical technique was used to monitor sweat gland activity on the forearm.

C. Computer Model Used to Process Subject Test Data

Fig. 2 presents the procedure used in this study to extract quantitative sweat rate values. To retrieve sweat rate values from the temperatures measured experimentally at the location of the sweat glands T_d and at a reference location T_r, a basic thermodynamics model was developed. This simple model can be divided into two parts: i) modeling the heat transfer phenomena taking place within the skin as well as at its boundaries and ii) modeling the evaporative cooling of the sweat droplet. As the

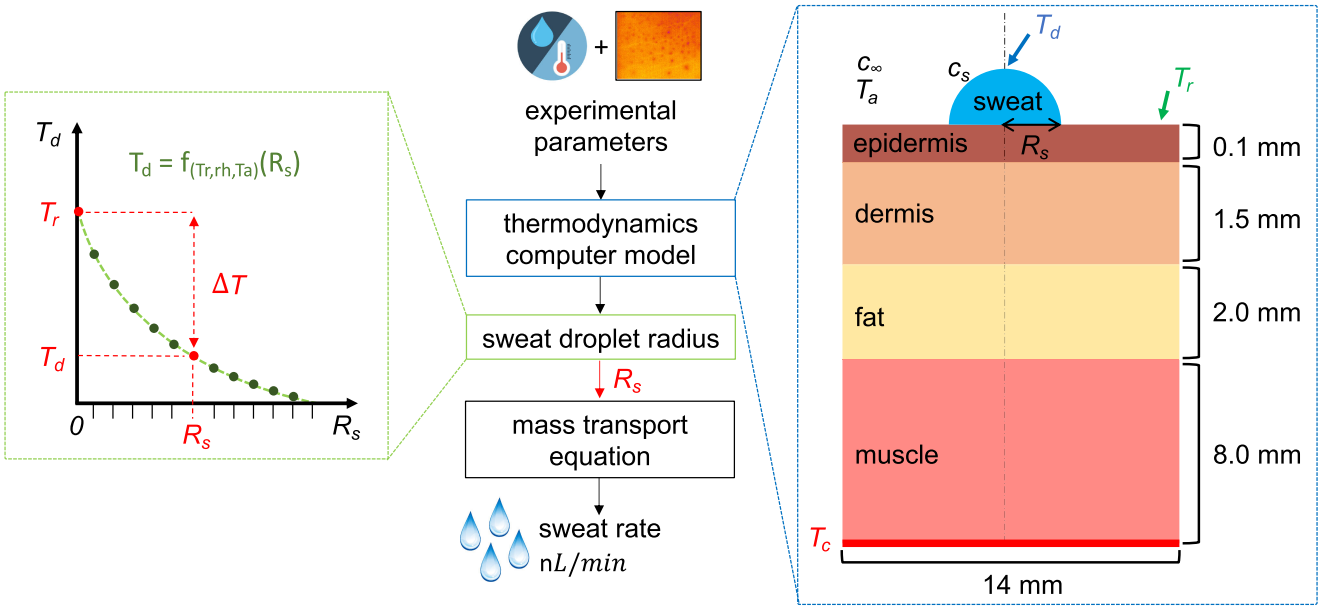

Fig. 2. Extraction of quantitative sweat rate value. An experimental parameters set (T_d, T_r, T_a, T_c, and rh) was used in combination with a FEM model [11] to determine sweat droplet radius R_s. From R_s, sweat rate can be computed using (2).

problem does not possess a fully analytical solution, a computer model was developed using the finite-element method (FEM)-based simulation software COMSOL Multiphysics version 5.6 (COMSOL Multiphysics GmbH, Zurich, Switzerland).

The thermodynamics model of the skin used in this study has been previously reported [11]. In short, the skin was considered as a multilayer system consisting of the epidermis, the dermis (reticular and papillary), a fat layer, and a muscle layer. The Penne's bioheat equation was used to describe the influence of blood perfusion on the skin temperature distribution in terms of volumetrically distributed heat sources. The temperature was fixed at the bottom of the muscle layer and was set to be constant to equal the body core temperature.

In the computer model, sweat was considered to be water. The shape of the sweat droplet at the skin surface is strongly dependent on the contact angle of the droplet. The contact angle itself is strongly dependent on the skin surface and was therefore difficult to assess. Previous studies ([14], [15]) estimated that the contact angle varies from 78 °C to 118 °C depending on whether the droplet is 'advancing' (78 °C) or 'receding' (118 °C) from the pore. Because of these considerations, we reasonably assumed a perfectly half spherical droplet with radius R_s corresponding to a fixed contact angle of 90 °C. Cooling of the sweat droplet (and ultimately the skin surface) is achieved via radiation, convection and evaporation. The surface of the sweat droplet is subject to natural, unforced convection and radiation. The evaporation cooling power in Watt per square meter can be stated as [16]

$$Q_0 = 2\pi R_s D_w (c_s - c_\infty) \Delta H_{vap}\,, \tag{1}$$

where D_w is the diffusion coefficient (m^2/s) and c is the absolute concentration of water vapor (kg/m^3) at the surface of the droplet c_s and away from it c_∞. ΔH_{vap} is the latent heat of vaporization of water. D_w, c and ΔH_{vap} are temperature dependent quantities. Nonetheless, in the range of temperatures involved, we can neglect variations of the latent heat of vaporization as well as the diffusion coefficient. In the model, ΔH_{vap} was set to 2.4298×10^6 J/kg and D_w was set to 0.234733×10^{-4} m^2/s. The absolute concentration of water vapor varies significantly with temperature and relative humidity [16].

TABLE I
PARAMETERS USED FOR COMPUTER MODELING. ALTHOUGH THE OJECTIVE OF THE MODEL WAS TO COMPUTE THE DROPLET TEMPERATURE, IT WAS ENTERED AS AN EXTERNAL PARAMETER IN THE LATENT HEAT OF VAPORIZATION

Parameters:	Value	Units
Droplet radius R_s	25 - 1000	µm
Ambient temperature T_a	18 - 23	°C
Core body temperature T_c	34 - 39	°C
Relative humidity rh	10 - 90	%
Temperature droplet T_d	27 - 32	°C

A parametric run was achieved varying different parameters such as the ambient temperature, relative humidity or core body temperature. Table I presents the parameters which were varied in this study. For each parameter set, the droplet temperature T_d was numerically evaluated as a function of the droplet radius R_s (see Fig. 2). A bi-exponential function was used to fit the numerical values generated, taking into account that at $R_a = 0$ the temperature of the sweat droplet equals the reference temperature T_r. The measured temperature of the droplet T_d allows one to compute the sweat radius R_s. The sweat rate can be calculated using

$$\frac{\partial V}{\partial t} = \frac{2\pi R_s D_w (c_s - c_\infty)}{\rho_w}\,. \tag{2}$$

Interestingly, some parameters such as T_c only influence the skin temperature and will lead to a vertical offset of the droplet temperature versus droplet radius curve. As a result, it was

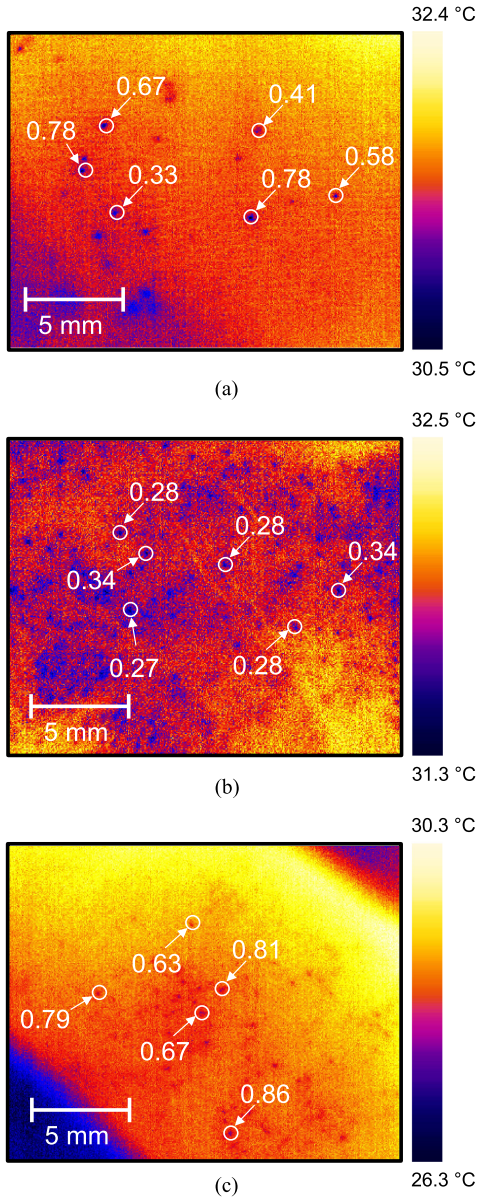

Fig. 3. Example of sweat quantification on three different body parts (forearm, palm and finger). Sweat rates were labeled in white and given in nL · min^{-1}. The method allowed quantification of several sweat glands individually and simultaneously. (a) Location: forearm; gender: male; $T_a = 25.1\,^{\circ}$C; $rh = 51\%$. (b) Location: palm; gender: male; $T_a = 25.1\,^{\circ}$C; $rh = 51\%$. (c) Location: finger; gender: male; $T_a = 22.3\,^{\circ}$C; $rh = 41\%$.

unnecessary to measure the subject core body temperature to retrieve the sweat rate.

III. Results and Discussion

A. Sweat Rate Quantification on Different Regions of the Body

To test our method, several thermograms obtained on different body parts were investigated during exercise stimulated sweating (see Fig. 3). On each thermogram, the sweat glands were easily identified as cold/dark spots and their density could be estimated. As expected, density was much higher on the palm than on the forearm [17]. On each thermogram, the minimal temperature at the location of 6 sweat glands was measured together with a reference temperature taken from an area with no sweat glands. The temperature difference was used to compute the radius of the sweat gland and the resulting sweat rate (in nL/min) for a defined ambient temperature and relative humidity (see Fig. 3). The camera used in this study had a noise equivalent temperature difference of 40 mK; this means that on a single image, the minimal temperature difference that could be measured was $0.004\,^{\circ}$C, leading to potentially low sweat rate measurements. For example, for an ambient temperature of $20\,^{\circ}$C, a relative humidity of 40%, and a skin surface temperature of $32\,^{\circ}$C (T_r), the minimal sweat rate measurable was 0.0185 nL/min. If the skin temperature was lower (due to lower perfusion or lower core body temperature), for example $T_r = 27\,^{\circ}$C, the minimal sweat rate measurable would be 0.0133 nL/min. On the other hand, there is no theoretical limitation for the measurement of high sweat rates; however, practically, when a large volume of sweat is produced, the temperature of the whole measurement area drops and the individual sweat glands cannot be identified accurately.

B. Comparison of Sweat Pulsation Behavior During Natural Sweating and Chemically Stimulated Sweating

The optical method can also be used to observe sweat pulsation. It has been reported that 'natural sweating' is not a continuous process but a pulsatile one [18]. The method proposed in this paper is perfectly adapted to the investigation of sweat pulsation. Unlike other methods ([1]–[3], [19]), it is a non-contact approach that does not affect the skin surface. The infrared camera is fast enough to investigate the range of frequencies involved.

Fig. 4 presents thermograms of sweat gland activity over time. Three thermograms are displayed at 0 s, 37 s and 55 s. At 0 s, T_{d1} was still active, but T_{d2} and T_{d3} were not. T_{d3} became active at 35 s followed by T_{d2} at 50 s. Due to the relatively short measurement time in this preliminary study (100 s), it was impossible to see the repetition of the sweat glands' pulsatile activity. Nonetheless, all investigations performed using exercise stimulated sweating demonstrated such pulsatile behavior. The temperature drop observed during these pulses is further validated by past sweat studies. Data from multiple studies verify that the drop in skin temperature due to sweat droplets is typically around 1-2 degrees [20]–[22]. In addition, an interesting fact to note is that sweating seems to become much more profuse as the skin temperature reaches $35\,^{\circ}$C and begins to slow down/stop when the skin temperature reaches $33\,^{\circ}$C, further validating the results in this study [23]. A portable experimental setup minimizing involuntary movements and implementing movement compensation algorithms together with automatic sweat gland detection is in development. Further studies will be performed with such a device to investigate which factors influence the duration of the sweat rate pulse and its frequency.

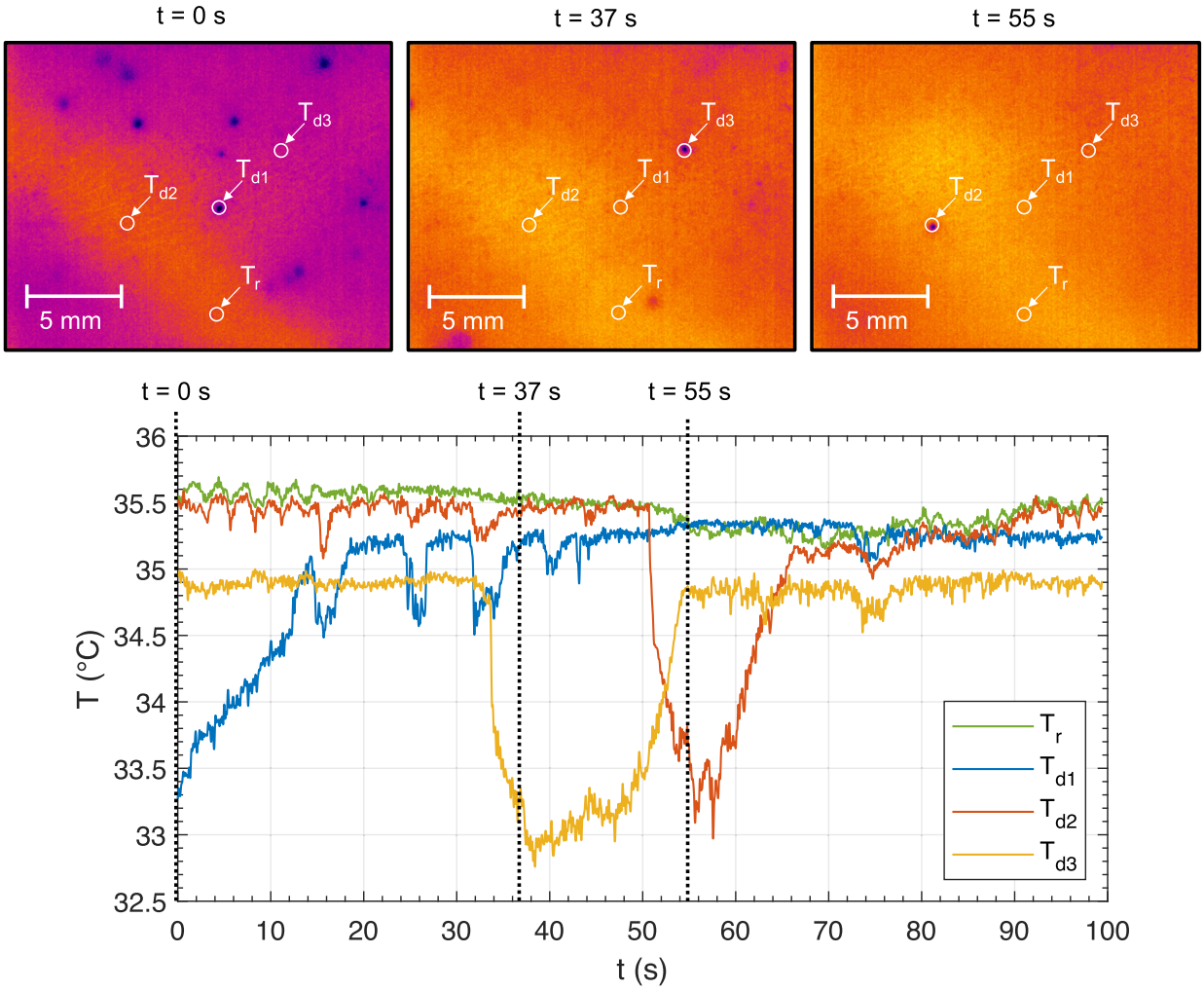

Fig. 4. Monitoring of sweat pulsation. We monitored three sweat glands (T_{d1}, T_{d2}, T_{d3}) and reference area T_r located on the forearm. The transient temperatures were recorded for 100 seconds.

An interesting item to be noted was that in the case of chemically induced sweating, the sweat glands appear to be continuously active, and no pulsation was observed. This lack of pulsation is extremely interesting, and speculations as to its mechanism will be discussed in the next section.

C. Investigation of Pulsatile Sweating Mechanism

To understand the reason that exercise stimulated sweating, or 'natural sweating', is pulsatile but chemically stimulated sweat is not, one must first understand the physiological mechanism behind natural sweating. There are two natural pathways that exist which cause eccrine glands to sweat. The first of these pathways is caused by exercise, or heat, and will be referred to as thermal sweating (and is the natural pathway examined in this study). The sweating mechanism begins with bursts of Skin Sympathetic Nerve Activity (SSNA). These bursts are brief (milliseconds) rises in nerve activity which act on receptors in the skin, causing eccrine glands to excrete sweat. These bursts of nerve activity have been well documented in several studies and seem to have high correlation with sweat expulsion [18], [24]–[27]. Most SSNA bursts have a very small amplitude, and occur at a much higher frequency than sweat expulsion pulses. This is because only larger amplitude bursts (or extremely rapidly occurring smaller bursts) seem to cause sweat expulsion, and these larger amplitude bursts occur much less frequently. Sweat expulsion typically occurs about three seconds after an initial large burst (or group of smaller bursts). The larger the amplitude of SSNA burst, the more sweat is typically expelled from the pore during that pulse [18]. In thermal sweating, the SSNA bursts cause acetylcholine to be released, which primarily stimulates M3 muscarinic receptors in the skin, inducing sweating [28]–[31]. As the core body temperature and skin temperature increase, the rate of SSNA bursts increases. If the bursts become rapid enough, sweating can begin to look continuous to the naked eye as the nerve activity burst peaks begin to fuse together, even though the sweating remains truly pulsatile. In contrast, the other pathway which exists for natural sweating is triggered by stress, fright, or other strong emotion, and will be referred to as stress sweating. Stress sweating is distinct from thermal sweating in that different receptors are stimulated and the sweating itself is much less likely to appear continuous. In the stress sweating pathway, the

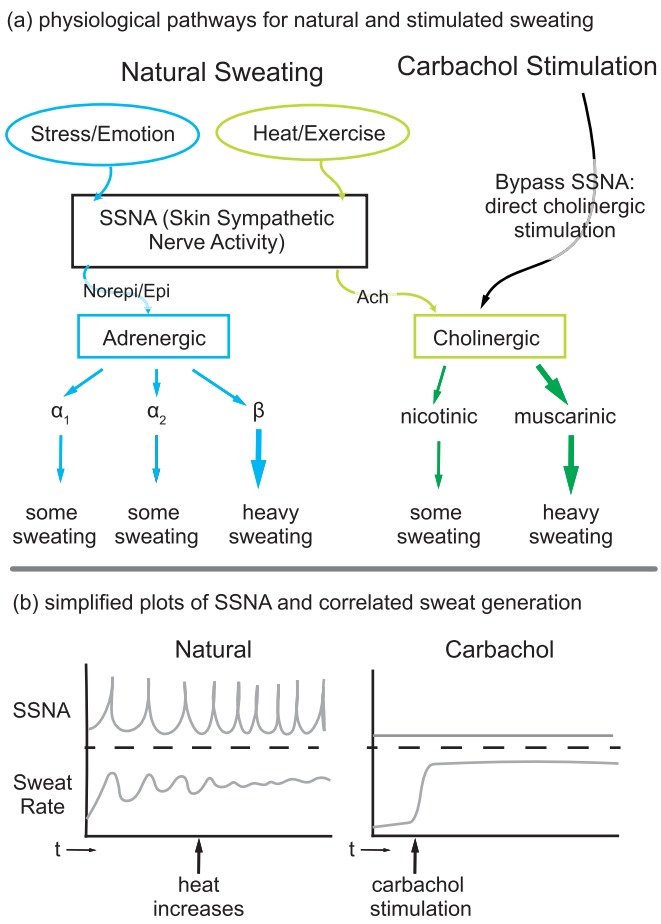

Fig. 5. The major pathways for natural and chemically stimulated sweating [30], [31]. Chemically stimulated sweating activates the same receptors as thermal sweating [12], but results in constant sweating rather than pulsatile sweating due to the constant activation of cholinergic receptors. (a) physiological pathways for natural and stimulated sweating. (b) simplified plots of SSNA and correlated sweat generation.

SSNA bursts cause epinephrine and norepinephrine (primarily norepinephrine) to be released rather than acetylcholine, which in turn stimulate adrenergic receptors near the skin to induce sweating.

The mechanisms of chemically stimulated sweating are slightly different than that of the two natural sweating pathways. When carbachol is delivered into the skin (either by iontophoresis or injection), it stimulates muscarinic and nicotinic receptors, similarly to acetylcholine during natural thermal sweating. However, rather than the periodic release of acetylcholine, which is limited by the SSNA bursts, the carbachol continuously activates the receptors due to its extremely slow metabolism by acetylcholinesterase. The constant stimulation of the receptors causes a steady stream of sweat to be excreted from the pore, rather than the pulsatile sweating seen in natural sweating. A summary of the natural sweating pathways as well as the mechanism of chemically stimulated sweating can be seen in Fig. 5. Unlike previous approaches for sweat rate measurement, characterization of pulsatile versus non-pulsatile sweating is something only observable with this new optical approach.

D. Discussion on Potential Applications for Optical Method

Now that the most likely mechanisms behind natural and chemically stimulated sweating are understood, what effect does this new optical sweat rate measurement technique and new observations of sweat pulsation have on real-world applications? We break the discussion here into two main topics: i) improved disease diagnosis, and ii) potential utility for wearable sensors.

Hyperhidrosis is a condition in which a person has excessive sweating in certain areas of the body, commonly the palms, axillae, and soles of the feet. Hypohidrosis, on the other hand, is a condition in which a person experiences decreased sweating, or in the case of anhidrosis, no sweating at all. The most common methods used to diagnose both hyper and hypohidrosis are subjective in nature and involve frequency/location of sweating as well as family history [32]–[34]. The optical method discussed in this article can be used alone as a more accurate tool for the diagnosis of these disorders or could also be used to enhance the accuracy and interpretation of existing tests. Rather than using more simplified methods such as gravimetric testing to determine the amount of sweating, the camera data would provide a more accurate, continuous quantification of sweat rate, which could be used to determine the severity of the disorder. In addition, the optical technique could also be used to monitor the effectiveness of various treatment methods for hyper and hypohidrosis being used in patient care.

This optical technique for sweat rate measurement could also be potentially useful for diagnosis of peripheral nerve degeneration by improving diagnostic methods such as the Quantitative Sudomotor Axon Reflex Test (QSART). QSART is a testing method which uses iontophoresis to chemically stimulate sweating (similar to the carbachol stimulation used in this article) in the peripheral limbs, typically the legs and forearm [5]. A low sweat output is indicative of peripheral nerve degeneration. The method presented in this article would allow the clinician to know the sweat gland density of the area and the exact sweat output of each gland. It would also allow the physician to measure sweat output at a ‘reference’ site which would not have nerve degeneration to determine the severity of their condition.

Another disease which could benefit from this technology is Cystic Fibrosis (CF). This disease is typically diagnosed in infants by measuring chloride concentration in their sweat. However, the sweat tests used for diagnosis use gravimetric methods to determine average sweat generation rate over a large patch of skin (several cm^2). High concentrations of chloride (the main indicator of CF) may not only be caused by CF but also by a low number of active sweat glands. This is because increased sweat rate by individual sweat glands results in higher chloride concentrations due to the inability for the gland to reabsorb the ions before escaping the pore. Therefore, individuals who have lower overall sweat gland density, but higher sweat generation rates may have higher chloride concentrations in their sweat which presents falsely as CF. Having the ability to monitor individual sweat glands using this optical method will lead to more accurate CF diagnosis.

It is important to discuss the possible issues which may arise due to stimulated sweat. Sweat stimulation may cause changes in local levels of metabolites, such as lactate. Since lactate is a byproduct of anaerobic activity, an increase in sweat gland activity will locally increase levels of lactate which do not properly correlate with levels of lactate in the body. It is also possible that changes in certain analytes may cause indirect changes in concentrations of other biomarkers in sweat by affecting the sweat osmolality or by affecting the ability of certain markers to diffuse/partition into the lumen [35]. However, effects such as these due to sweat stimulation are not well understood and need to be investigated as wearable sweat sensing platforms develop further.

However, chemically induced sweating also has many positive effects on sweat sensing. It is largely known that directly placing the sensor on the skin will likely cause issues such as contamination, evaporation, and sweat discontinuity. Chemically stimulated sweating helps to control for these issues, as the steady stream of sweat is guaranteed to keep the sensor wet and will also therefore reduce noise in the signal. Stimulated sweat is also advantageous because it may reduce noise when using enzymatic sensors, which with pulsatile sweat could give false pulsatile sensor readings due to the sensor signal being dependent on the flux of the analyte to the enzyme layer [36], [37]. A higher incoming flow rate may result in falsely high concentrations (if flow rate is $3\times$ faster, the concentration will appear $3\times$ higher than the actual bodily concentration). Having a continuous stream of sweat with a consistent flow rate, as is seen with chemically stimulated sweating, would avoid this phenomenon and improve the accuracy of sweat condition diagnosis.

Finally, due to the recent rapid development of miniaturized infrared cameras exhibiting sufficient spatial resolution (for example the Lepton 3 cores, Teledyne FLIR, Portland OR, USA exhibiting 160×120 pixels or Mosaic core, Seek Thermal, Santa Barbara CA, USA exhibiting 340×240 pixels), the approach presented in this study could be integrated into wearable devices allowing the monitoring of sweat glands over longer periods.

IV. Conclusion

The method of sweat rate measurement described in this article is capable of measuring individual sweat gland activity, rather than average quantities over a general area as is done with current methods which use skin humidity or the galvanic skin response. These individual measurements may allow for more accurate diagnosis of conditions such as CF, peripheral nerve degeneration, and hyper/hypohidrosis. This optical method also enables the observation of sweat gland pulsatile activity by looking at natural sweat stimulation versus chemically stimulated sweating. Interestingly, it was observed that chemically stimulated sweating produced a steady stream of sweat which was expelled from the gland, most likely due to the constant stimulation of muscarinic receptors by carbachol. This behavior was distinctly different from the observed naturally stimulated sweating, which produced pulsatile sweat expulsion due to the the intermittent stimulation of receptors by the sympathetic nervous system. The constant expulsion of sweat during chemically stimulated sweating may provide significant benefits for certain biosensing applications, such as for enzymatic sensors; however, it is possible that chemically stimulated sweating may alter local lactate levels, potentially leading to false sweat/plasma correlations. Therefore, care should be taken to investigate this as well as other possible confounding variables if using chemically stimulated sweating. To conclude, the non-contact optical method of sweat rate measurement described in this article could improve sweat biosensing by providing valuable insight into sweat gland mechanisms, and could potentially increase the accuracy of sweat disease diagnoses.

Acknowledgment

The author would like to thank Philip Marmet, Christoph Kirsch and Marco Lattuada for fruitful discussions about the computer model used in this study. M. B. is a former DIZH Fellow and acknowledges support from ZHAW digital.

References

[1] J. K. Sim, S. Yoon, and Y.-H. Cho, "Wearable sweat rate sensors for human thermal comfort monitoring," *Sci. Rep.*, vol. 8, no. 1, 2018, Art. no. 1181.
[2] J. D. Montagu and E. M. Coles, "Mechanism and measurement of the galvanic skin response," *Psychol. Bull.*, vol. 65, no. 5, pp. 261–279, 1966.
[3] M. Sharma, S. Kacker, and M. Sharma, "A brief introduction and review on galvanic skin response," *Int. J. Med. Res. Professionals*, vol. 2, no. 6, pp. 13–17, 2016.
[4] A. Green and J. Kirk, "Guidelines for the performance of the sweat test for the diagnosis of cystic fibrosis," *Ann. Clin. Biochem.*, vol. 44, no. 1, pp. 25–34, 2007.
[5] A. Riedel *et al.*, "Quantitative sudomotor axon reflex test (QSART): A new approach for testing distal sites," *Muscle Nerve*, vol. 22, no. 9, pp. 1257–1264, 1999.
[6] F. Birklein *et al.*, "Sudomotor function in sympathetic reflex dystrophy," *Pain*, vol. 69, no. 1, pp. 49–54, 1997.
[7] R. A. Benson *et al.*, "Diagnosis and management of hyperhidrosis," *BMJ*, vol. 347, 2013, Art. no. 6800.
[8] K. Y. Chia and H. L. Tey, "Approach to hypohidrosis," *J. Eur. Acad. Dermatol. Venereol.*, vol. 27, no. 7, pp. 799–804, 2013.
[9] N. B. Morris *et al.*, "A comparison between the technical absorbent and ventilated capsule methods for measuring local sweat rate," *J. Appl. Physiol.*, vol. 114, no. 6, pp. 816–823, 2013.
[10] M. Charlton *et al.*, "The effect of constitutive pigmentation on the measured emissivity of human skin," *PLoS One*, vol. 15, no. 11, 2020, Art. no. e0241843.
[11] M. Bonmarin and F.-A. Le Gal, "Lock-in thermal imaging for the early-stage detection of cutaneous melanoma: A feasibility study," *Comput. Biol. Med.*, vol. 47, pp. 36–43, 2014.
[12] P. Simmers *et al.*, "Prolonged and localized sweat stimulation by iontophoretic delivery of the slowly-metabolized cholinergic agent carbachol," *J. Dermatological Sci.*, vol. 89, no. 1, pp. 40–51, 2018.
[13] Z. Sonner *et al.*, "Integrated sudomotor axon reflex sweat stimulation for continuous sweat analyte analysis with individuals at rest," *Lab Chip*, vol. 17, no. 15, pp. 2550–2560, 2017.
[14] L. Hou *et al.*, "Artificial microfluidic skin for in vitro perspiration simulation and testing," *Lab Chip*, vol. 13, no. 10, pp. 1868–1875, 2013.
[15] A. Mavon, "The wetting properties of human skin," in *Contact Angle, Wettability Adhesion*, K. L. Mittal Ed., vol. 2. Ed. Boca Raton (FL): CRC Press, 2002, pp. 469–479.
[16] H. Y. Erbil, "Evaporation of pure liquid sessile and spherical suspended drops: A review," *Adv. Colloid Interface Sci.*, vol. 170, no. 1, pp. 67–86, 2012.
[17] P. A. Low, *Primer on the Autonomic Nervous System*, 3rd ed. New York, NY, USA: Academic Press, 2012, ch. 51, pp. 249–251.

[18] J. Sugenoya *et al.*, "Identification of sudomotor activity in cutaneous sympathetic nerves using sweat expulsion as the effector response," *Eur. J. Appl. Physiol. Occup. Physiol.*, vol. 61, no. 3, pp. 302–308, 1990.
[19] A. Brueck *et al.*, "A real-time wireless sweat rate measurement system for physical activity monitoring," *Sensors*, vol. 18, no. 2, 2018, Art. no. 533.
[20] S. Nakata *et al.*, "Wearable, flexible, and multifunctional healthcare device with an ISFET chemical sensor for simultaneous sweat pH and skin temperature monitoring," *ACS Sensors*, vol. 2, no. 3, pp. 443–448, 2017.
[21] J. Libert, V. Candas, and J. Vogt, "Effect of rate of change in skin temperature on local sweating rate," *J. Appl. Physiol.*, vol. 47, no. 2, pp. 306–311, 1979.
[22] N. Kondo *et al.*, "The effect of change in skin temperature due to evaporative cooling on sweating response during exercise," *Int. J. Biometeorol.*, vol. 40, no. 2, pp. 99–102, 1997.
[23] T. Benzinger, "Clinical temperature - new physiological basis," *J. Amer. Med. Assoc.*, vol. 209, no. 8, pp. 1200–1206, 1969.
[24] G. Bini *et al.*, "Thermoregulatory and rhythm-generating mechanisms governing the sudomotor and vasoconstrictor outflow in human cutaneous nerves," *J. Physiol.*, vol. 306, no. 1, pp. 537–552, 1980.
[25] J. Sugenoya *et al.*, "Vasodilator component in sympathetic nerve activity destined for the skin of the dorsal foot of mildly heated humans," *J. Physiol.*, vol. 507, no. 2, pp. 603–610, 1998.
[26] Y.-I. Kamijo, K. Lee, and G. W. Mack, "Active cutaneous vasodilation in resting humans during mild heat stress," *J. Appl. Physiol.*, vol. 98, no. 3, pp. 829–837, 2005.
[27] M. Shibasaki and C. G. Crandall, "Mechanisms and controllers of eccrine sweating in humans," *Front. Biosci.*, vol. 2, pp. 685–696, 2010.
[28] K. Wilke *et al.*, "A short history of sweat gland biology," *Int. J. Cosmetic Sci.*, vol. 29, no. 3, pp. 169–179, 2007.
[29] M. Harker, "Psychological sweating: A systematic review focused on aetiology and cutaneous response," *Skin Pharmacol. Physiol.*, vol. 26, no. 2, pp. 92–100, 2013.
[30] H. Murota *et al.*, "Sweat, the driving force behind normal skin: An emerging perspective on functional biology and regulatory mechanisms," *J. Dermatological Sci.*, vol. 77, no. 1, pp. 3–10, 2015.
[31] Y. Hu *et al.*, "Neural control of sweat secretion: A review," *Brit. J. Dermatol.*, vol. 178, no. 6, pp. 1246–1256, 2018.
[32] H. W. Walling, "Clinical differentiation of primary from secondary hyperhidrosis," *J. Amer. Acad. Dermatol.*, vol. 64, no. 4, pp. 690–695, 2011.
[33] F. C. T. Smith, "Hyperhidrosis," *Surg. (Oxford)*, vol. 31, no. 5, pp. 251–255, 2013.
[34] A.-A. D. Lakraj, N. Moghimi, and B. Jabbari, "Hyperhidrosis: Anatomy, pathophysiology and treatment with emphasis on the role of botulinum toxins," *Toxins*, vol. 5, no. 4, pp. 821–840, 2013.
[35] Z. Sonner *et al.*, "The microfluidics of the eccrine sweat gland, including biomarker partitioning, transport, and biosensing implications," *Biomicrofluidics*, vol. 9, no. 3, 2015, Art. no. 031301.
[36] M. Chung, G. Fortunato, and N. Radacsi, "Wearable flexible sweat sensors for healthcare monitoring: A review," *J. Roy. Soc. Interface*, vol. 16, no. 159, 2019, Art. no. 20190217.
[37] P. Salvo *et al.*, "A wearable sensor for measuring sweat rate," *IEEE Sensors J.*, vol. 10, no. 10, pp. 1557–1558, Oct. 2010.